



## UWS Academic Portal

Shang, Fengjie; Li, Qinlan; Shi, Yongjing; Liu, Haiding; Song, Shigeng

*Published in:*  
Gongneng Cailiao/Journal of Functional Materials

*DOI:*  
[10.3969/j.issn.1001-9731.2021.06.010](https://doi.org/10.3969/j.issn.1001-9731.2021.06.010)

Published: 30/06/2021

*Document Version*  
Peer reviewed version

[Link to publication on the UWS Academic Portal](#)

*Citation for published version (APA):*  
Shang, F., Li, Q., Shi, Y., Liu, H., & Song, S. (2021). . *Gongneng Cailiao/Journal of Functional Materials*, 52(6), 06076-06083. <https://doi.org/10.3969/j.issn.1001-9731.2021.06.010>

### General rights

Copyright and moral rights for the publications made accessible in the UWS Academic Portal are retained by the authors and/or other copyright owners and it is a condition of accessing publications that users recognise and abide by the legal requirements associated with these rights.

### Take down policy

If you believe that this document breaches copyright please contact [pure@uws.ac.uk](mailto:pure@uws.ac.uk) providing details, and we will remove access to the work immediately and investigate your claim.

# 固体氧化物燃料电池阴极材料的研究进展

尚凤杰<sup>1</sup>, 李沁兰<sup>1</sup>, 石永敬<sup>1†</sup>, 戴炜<sup>1</sup>, 刘海定<sup>2</sup>, Shigeng Song<sup>3</sup>

(1. 重庆科技学院 冶金与材料工程学院, 重庆 401331; 2. 重庆材料研究院, 重庆 401331; 3. Institute of Thin Films, Sensors and Imaging, School of Engineering and Computing, University of the West of Scotland, Paisley PA1 2BE, UK)

**摘要:** 阴极材料是固体氧化物燃料电池的重要组成。提高阴极材料的电子/离子电导率、降低极化电阻是使 SOFC 低温化运行、延长电池使用寿命的重要方法。阴极材料的高电子电导性促使钙钛矿结构氧化物在阴极材料的研究领域占据主导地位。本文综述了钙钛矿结构阴极、尖晶石结构阴极和 Ruddlesden-popper 型结构阴极材料的研究进展, 并展望了未来阴极材料的发展方向。

**关键词:** 固体氧化物燃料电池; 阴极材料; 钙钛矿氧化物; 研究进展

中图分类号: TM911.4

文献标识码: A

## 0 引言

随着社会文明的发展和世界人口的迅速增长, 人类生活对能源的需求也在持续增长。化石燃料作为主要的能源来源, 为我们的社会生活提供了大量的资源。然而, 化石燃料的过度消耗产生了大量的二氧化碳 (CO<sub>2</sub>) 和杂质 (SO<sub>2</sub>、NO<sub>x</sub>), 引起了人们对环境污染和气候变化的担忧, 对我们社会文明的健康发展造成威胁<sup>[1-5]</sup>。因此, 为了实现可持续发展的未来, 迫切需要可再生能源和绿色能源转换技术<sup>[6]</sup>。固体氧化物燃料电池 (SOFC) 的转换效率高达 85%, 而且具有燃料灵活性大、低成本、安全稳定和大幅度降低 CO<sub>2</sub> 排放量等优点, 在能量转换、存储等领域具有巨大的发展前景<sup>[7,8]</sup>。SOFC 的主要由阴极、阳极和固体电解质三部分构成<sup>[9-30]</sup>。其中, 阴极是氧气发生还原反应的场所<sup>[31]</sup>。在阴极上, 氧分子吸附解离后得到电子被还原成氧离子:  $O_2 + 4e^- \rightarrow 2O^{2-}$ 。商业化的 SOFC 中, 最常见的组合是 LSM/YSZ/Ni-YSZ, 但氧化钪稳定氧化锆 (YSZ) 的使用温度居高不下。高温工作虽然有利于电极反应, 然而长时间的高温状态会加速电池性能的衰减, 极大地降低电池的使用寿命。因此降低其运行温度是 SOFC 发展的必然

---

收到初稿日期: 2021-01-21

收到修改稿日期: 2021-03-02

通讯作者: 石永敬, 博士/副教授; Email: [yjshi@126.com](mailto:yjshi@126.com);

作者简介: 尚凤杰 (1994-), 女, 河南开封人, 研究生, 师承石永敬副教授, 主要从事燃料电池材料的研究与开发。

趋势。本文作者回顾了 SOFC 阴极材料的研究进展，并展望了其未来的发展方向。

## 1 SOFC 阴极材料的基本要求

阴极是 SOFC 体系中最重要的重要组成部分之一，其材料需要满足的条件有：首先是较高的电子电导率 ( $>100\text{S}\cdot\text{cm}^{-1}$ )、一定的离子电导率。一定的离子电导率不但会提高催化反应，而且会增大氧离子的扩散能力，而较高的电子电导率可以显著降低欧姆损耗，提高转化效率。然后是对氧的电化学反应具有较高的催化活性、足够的孔隙率 (20%~40%) 以及良好的化学及物理稳定性。此外，还有一个重要的考虑因素是热膨胀系数 (TEC) 应能与相连的电解质相匹配。当电极材料与电解质材料的 TEC 不相容时，容易造成电池断裂、脱落，严重影响电池的稳定和正常运行<sup>[32]</sup>。

## 2 SOFC 阴极材料结构

SOFC 阴极材料种类繁多，根据晶体结构不同可将其分为钙钛矿结构、尖晶石结构和 Ruddlesden-popper 型结构材料，如图 1 所示。

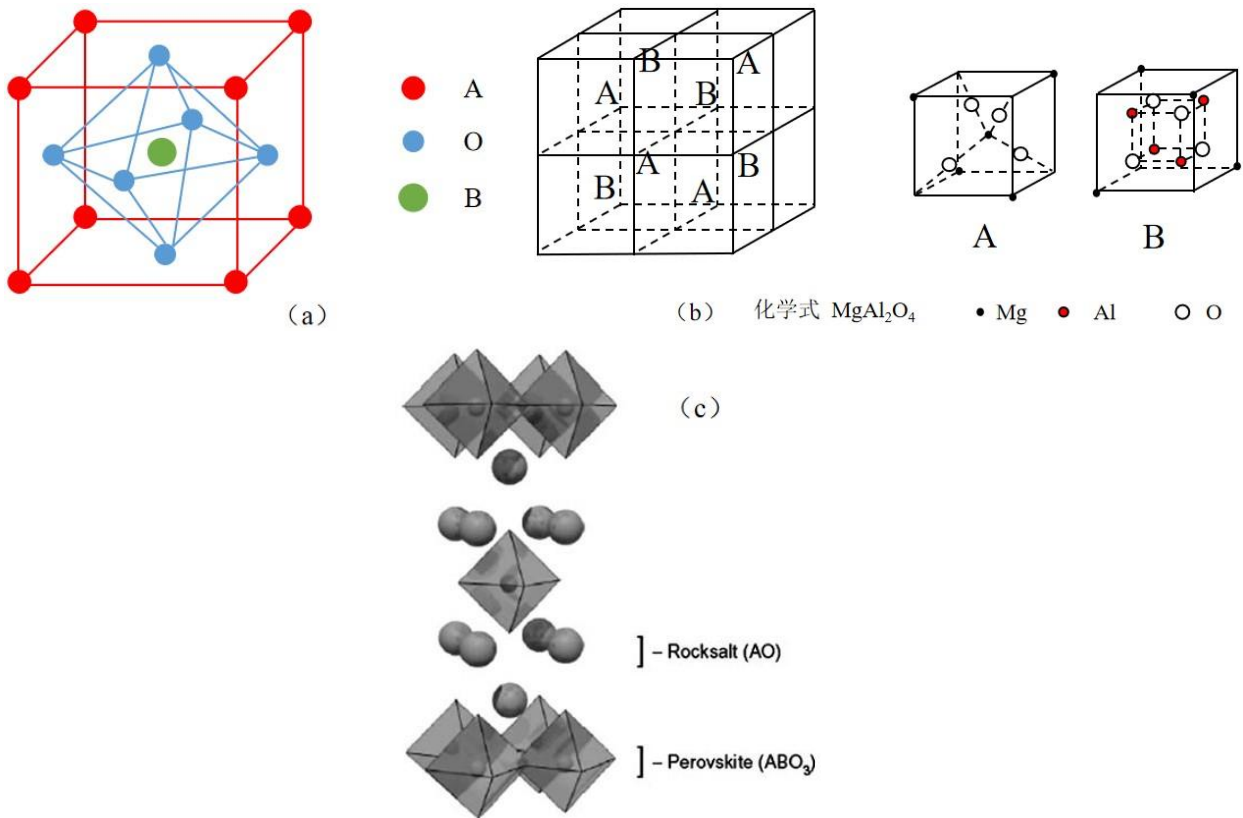


图 1. 常见阴极的结构种类：(a) 钙钛矿结构；(b) 尖晶石结构；(c) Ruddlesden-popper 型材料<sup>[33-45]</sup>

Fig 1. The structure types of common cathodes are as follows: (a) perovskite structure; (b) spinel structure; (c) Ruddlesden-popper type materials<sup>[33-45]</sup>

### 2.1 钙钛矿结构

钙钛矿结构氧化物在 SOFC 阴极材料中的应用非常广泛。标准的钙钛矿结构为立方晶系，可用  $ABO_3$  分子式表示，如图 1 (a) 所示，其中 A 位为稀土元素（如 La、Pr、Sm、Gd 和 Nd 等）和碱土金属元素（如 Sr、Ca 和 Ba 等），位于立方体的八个顶点，配位数为 12；B 位多是离子半径较小的过渡金属元素（如 Mn、Fe 和 Co 等），位于立方体的中心，配位数为 6；O 表示负 2 价的氧离子。影响钙钛矿催化活性的因素主要有两点：表面吸附氧和晶格氧。温度较低时，表面吸附氧起主要作用，由 B 位的过渡金属元素决定。温度较高时，晶格氧起作用，改变 A、B 位置的金属元素可以调节晶格氧的数量和活性，或者用二价阳离子部分替代晶格中 A、B 位离子产生晶格缺陷或晶格氧，提高催化活性。

### 2.1.1 $LaMnO_3$ 基阴极材料

锰酸镧 ( $LaMnO_3$ ) 是 SOFC 中应用比较成熟的一种钙钛矿型材料，对还原反应具有良好的电子导电性和高催化活性，并且结构稳定。在钙钛矿氧化物阴极材料研究中，通过在 A、B 位置上掺杂或置换金属阳离子（如 Ba、Ca、Co、Mg、Ni、Sr、Y 等），可以形成更多氧离子空位，增大离子电导率<sup>[46]</sup>。如当 Sr 掺杂  $LaMnO_3$  形成  $La_{1-x}Sr_xMnO_{3-\delta}$  (LSM) 时， $Sr^{2+}$  阳离子部分取代  $La^{3+}$ ，同时发生锰离子氧化，有效地增加空位浓度，提高离子电导率<sup>[46]</sup>。因此，LSM 一直是 SOFC 阴极材料中研究最多地一种。研究发现，采用浸渍法对阴极进行表面改进，可以增大反应活性区，提高阴极性能，浸渍过程如图 2 所示<sup>[47-52]</sup>。氧气在传统阴极上的反应活性区较小，导致其催化活性和离子电导率都比较低。在阴极中加入高离子导电相（如 YSZ），可以构建出电子-离子复合纳米阴极，还原反应延伸到整个复合阴极，增大了反应活性区。Ju 等人采用浸渍技术将 LSM 纳米颗粒沉积到多孔 YSZ 骨架上，制备了 LSM-YSZ 复合阴极。阴极电导率随 LSM 浸渍量的增加而提高。阴极极化电阻 ( $R_p$ ) 先随 LSM 浸渍的增加而减小，当负载约 4.5vol.% 时， $R_p$  有最小值  $0.569\Omega\cdot cm^2$ ，然后随浸渍的增加而增大，如图 3 所示<sup>[53]</sup>。这是因为当 LSM 纳米颗粒沉积在 YSZ 晶粒表面时，会产生 LSM-YSZ 反应活性区。随着 LSM 纳米颗粒数的增加，反应活性区增大， $R_p$  降低，当 YSZ 表面被 LSM 颗粒充分覆盖时，反应活性区达到峰值， $R_p$  有最小值。浸渍量进一步增加时，多余的 LSM 纳米颗粒会阻碍气体的传输孔道，从而降低电化学反应活性区，增大  $R_p$ 。此外，将 SDC 浸渍到 LSM 上可以制备 LSM-SDC 复合阴极。LSM-SDC 阴极的面积比电阻 (ASR) 随 SDC 浸渍量的增多而逐渐增大，浸渍量为 50wt.% 时，有最小的 ASR 值  $0.23\Omega\cdot cm^2$ 。当 SDC 浸渍量进一步增多时，阴极 ASR 反而增大。这可能是由于 SDC 含量增多，孔隙率下降，从而增加浓度极化。

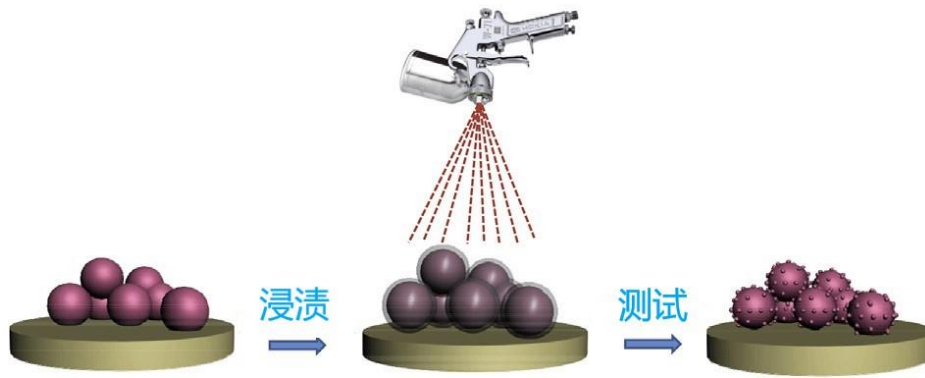


图 2. 喷雾浸渍工艺和阴极的形态变化<sup>[48]</sup>

Fig 2. Spray impregnation process and morphology change of cathode<sup>[48]</sup>

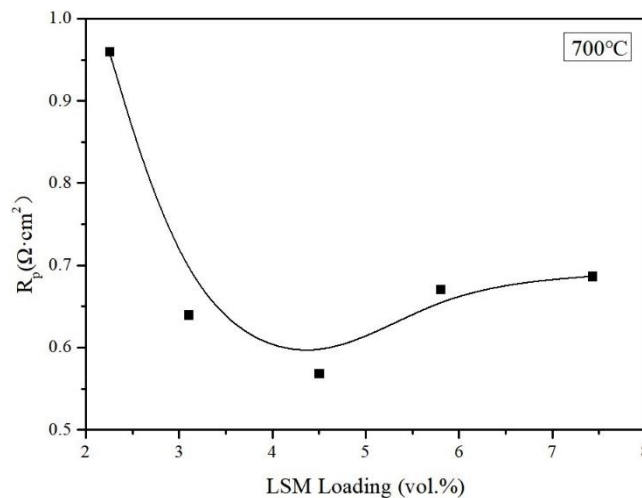


图 3. 700°C时，LSM 负载对极化电阻 ( $R_p$ ) 的影响<sup>[53]</sup>

Fig 3. Effect of LSM loading on polarization resistance ( $R_p$ ) at 700°C<sup>[53]</sup>

### 2.1.2 LaCoO<sub>3</sub> 基阴极材料

钴酸镧 (LaCoO<sub>3</sub>) 也是 SOFC 中一种常用的钙钛矿结构材料，在相同的条件下，LaCoO<sub>3</sub> 比 LaMnO<sub>3</sub> 的电导率大很多。掺杂 Sr 的 LaCoO<sub>3</sub> (La<sub>1-x</sub>Sr<sub>x</sub>CoO<sub>3-δ</sub>, LSC) 在氧化环境中会形成大量的氧空位，增大氧扩散能力，提高离子电导率<sup>[54]</sup>。但是 LSC 材料并没有得到广泛的应用，原因是 Co 元素的出现使得 La 元素更易于从阴极层扩散至电解质层，并发生固相反应生成高电阻相的 La<sub>2</sub>Zr<sub>2</sub>O<sub>7</sub>，而且所有掺 Sr 的钴阴极材料在 800°C 时会和 YSZ 电解质反应生成 SrZrO<sub>3</sub> 绝缘相，导致极化电阻显著增大<sup>[55]</sup>。即 LSC 阴极与 YSZ 平台的电解质具有极强的反应性，LSC-YSZ 体系受到限制。为了对此进行控制，可以在阴极和电解质之间添加一个阻挡层（如 GDC、SDC），从而避免其他相的生成，但这种方法并不是很成功，因为 LSC 与 YSZ 存在较大的 TEC 失配问题。还有一种方法是用其他阳离子（如 Ni<sup>2+</sup>、Fe<sup>3+</sup>等）部分或全部取代 LSC 中的 Co<sup>3+</sup>。其中，La<sub>0.6</sub>Sr<sub>0.4</sub>Co<sub>0.2</sub>Fe<sub>0.8</sub>O<sub>3-δ</sub> (LSCF) 具有较高的电子和离子电导率及适用的热膨胀特性，是 SOFC 中研究广泛的阴极材料，其功率密度与 LSM 类似，但工作温度比 LSM 低。近

几年对 LSCF 基阴极 SOFC 性能的研究如表 1 所示。

表 1. LSCF 基阴极的电池性能

Table 1 Battery performance of LSCF based cathode

阴极材料	制备方法	温度 (°C)	功率密度 (mW·cm <sup>-2</sup> )	极化电阻 (Ω·cm <sup>2</sup> )	参考 文献
LSCF-SDC	浸渍	600		0.15	[56]
La <sub>0.6</sub> Ca <sub>0.4</sub> Co <sub>0.2</sub> Fe <sub>0.8</sub> O <sub>3-δ</sub> -SDC				0.16	
LSCF <sub>6482</sub>	喷雾浸渍	700	940	0.04	[48]
LSCF	溶胶凝胶	750		0.21	[57]
La <sub>0.57</sub> Ce <sub>0.03</sub> Sr <sub>0.4</sub> Co <sub>0.2</sub> Fe <sub>0.8</sub> O <sub>3</sub>				0.14	
La <sub>0.54</sub> Ce <sub>0.06</sub> Sr <sub>0.4</sub> Co <sub>0.2</sub> Fe <sub>0.8</sub> O <sub>3</sub>				0.09	
LSCF-Ce <sub>0.8</sub> Gd <sub>0.2</sub> O <sub>1.9</sub>	喷雾热解沉积	600	500	0.27	[58]
LSCF-Gd <sub>0.1</sub> Ce <sub>0.9</sub> O <sub>1.95</sub>	机械处理	800		0.08	[59]
		750		0.17	
		700		0.38	
		650		0.69	
LSCF	浸渍	550	46	4.93	[60]
33.7wt.% YSB-LSCF			103	2.04	
40.6wt.% YSB-LSCF			167	1.06	

LSCF: La<sub>0.6</sub>Sr<sub>0.4</sub>Co<sub>0.2</sub>Fe<sub>0.8</sub>; SDC: Ce<sub>0.8</sub>Sm<sub>0.2</sub>O<sub>1.9</sub>; YSB: Y<sub>0.25</sub>Bi<sub>0.75</sub>O<sub>1.5</sub>

### 2.1.3 LaFeO<sub>3</sub> 基阴极材料

铁酸镧 (LaFeO<sub>3</sub>) 钙钛矿也可以用作 SOFC 阴极, 但是 LaFeO<sub>3</sub> 的电导率并不高, 需要掺杂金属离子 (如 Sr) 以提高孔隙率, 增大电导率<sup>[61]</sup>。Kammer Hansen 研究了以 Ce<sub>1.9</sub>Gd<sub>0.1</sub>O<sub>1.95</sub> 为电解质的 (La<sub>1-x</sub>Sr<sub>x</sub>)<sub>0.99</sub>FeO<sub>3-δ</sub> (x=0、0.05、0.15、0.25、0.35、0.50、0.70) (LSF) 阴极的电化学性能<sup>[62]</sup>。(La<sub>1-x</sub>Sr<sub>x</sub>)<sub>0.99</sub>FeO<sub>3-δ</sub> 阴极的 TEC 随 Sr 含量的增加而增大。(La<sub>1-x</sub>Sr<sub>x</sub>)<sub>0.99</sub>FeO<sub>3-δ</sub> 阴极的 ASR 先随 Sr 含量的增加而减小, 当 Sr 含量 x=0.15 时, ASR 有最小值, 之后 ASR 随着 Sr 含量的继续增大而增大, 如图 4 所示。此外, 在 700°C 时, Sr 和 Ni 双掺杂的 La<sub>1-x</sub>Sr<sub>x</sub>Fe<sub>0.7</sub>Ni<sub>0.3</sub>O<sub>3-δ</sub> 阴极的电导率从 90S·cm<sup>-1</sup> (LSFN0) 增加到最大值 200S·cm<sup>-1</sup> (LSFN0.2), 然后下降<sup>[61]</sup>。这是因为电导率与掺杂剂含量有关, 适当的掺杂量可以增大电导率, 降低阻抗, 而过大的掺杂量则会提高浓度, 增大浓度极化电阻。

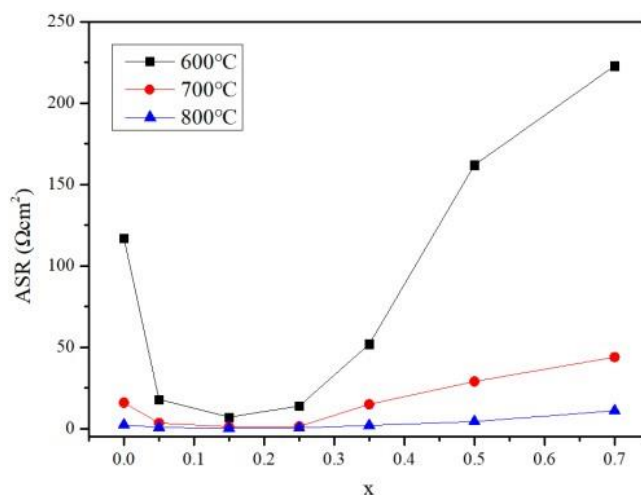


图 4.  $(La_{1-x}Sr_x)_{0.99}FeO_{3-\delta}$  ( $x=0, 0.05, 0.15, 0.25, 0.35, 0.50, 0.70$ ) 阴极的 ASR 与 Sr 含量的关系<sup>[62]</sup>

Fig 4. Relationship between ASR and Sr content of  $(La_{1-x}Sr_x)_{0.99}FeO_{3-\delta}$  ( $x=0, 0.05, 0.15, 0.25, 0.35, 0.50, 0.70$ ) cathode<sup>[62]</sup>

## 2.2 尖晶石结构

尖晶石 ( $AB_2O_4$ ) 型氧化物材料的性能主要是由二价 ( $Mg^{2+}$ 、 $Zn^{2+}$ 等)、三价 ( $Al^{3+}$ 、 $Co^{3+}$ 、 $Cr^{3+}$ 等) 离子的分布造成的。在  $AB_2O_4$  结构中, 氧离子按立方紧密堆积排列, 二价阳离子位于四面体空隙中, 三价阳离子位于八面体空隙中, 如图 1 (b) 所示。尖晶石材料具有化学稳定性强、高温下耐腐蚀性强以及热稳定性良好的优点, 作为阴极材料已受到广泛的关注<sup>[39, 40, 63-67]</sup>。例如,  $Mn_{1.5}Co_{1.5}O_4$  (MCO) 阴极材料, MCO 具有良好的热稳定性和结构稳定性, 以及较高的电子电导率, 是一种性能优异的 SOFC 阴极材料<sup>[68, 69]</sup>。与 MCO 阴极相比, SDC-MCO 复合阴极的电池性能明显下降。产生这个结果的主要原因是 MCO-SDC 复合阴极的电子电导率比 MCO 阴极低, 以致 MCO-SDC 复合阴极的电流收集困难。研究发现, 在 MCO-SDC 复合阴极上镀一层集流层可以显著改善电池性能。例如, 将具有良好混合电子-离子导电性的钙钛矿氧化物  $Sm_{0.5}Sr_{0.5}CoO_3$  涂覆到 MCO-SDC 复合阴极上, 其峰值功率密度比 MCO、MCO-SDC 阴极都高, 甚至显著高于同等条件下的 LSM-YSZ 阴极。孙克宁团队提出一种新的  $CuCo_2O_4$  尖晶石型阴极材料, 在 800、750 和 700°C 时的极化电阻分别为  $0.12$ 、 $0.25$  和  $0.4 \Omega \cdot cm^2$ , 峰值功率密度达  $972$ 、 $800$  和  $620 mW \cdot cm^{-2}$ <sup>[63]</sup>。 $CuCo_2O_4$  材料具有半导体特性, 电导率随着温度的升高而增加, 800°C 时的电导率为  $114 S \cdot cm^{-1}$ 。同时,  $CuCo_2O_4$  阴极与氧化钐稳定氧化锆 (SSZ) 电解质的 TEC 相近, 说明  $CuCo_2O_4$  材料与 SOFC 组件相匹配, 可以作为 SOFC 阴极材料长期运行。将  $CuCo_2O_4$  作为前驱体浸渍到多孔 SSZ 电解质中, 可以增大反应活性区, 降低极化电阻, 提高 SOFC 的电化学性能, 如图 5 所示<sup>[70]</sup>。在 800°C 时, 浸渍阴极的极化电阻降低至  $0.087 \Omega \cdot cm^2$ ,



是目前尖晶石结构材料的最佳性能。最近，Li 研究报道了  $\text{FeCo}_2\text{O}_{4-x}\text{Ce}_{0.8}\text{Sm}_{0.2}\text{O}_{1.9}$  ( $x=0、30、40、50、60、70\text{wt.}\%$ ) 复合氧化物作为 SOFC 阴极材料的性能研究<sup>[39]</sup>。 $\text{Ce}_{0.8}\text{Sm}_{0.2}\text{O}_{1.9}$  的加入对  $\text{FeCo}_2\text{O}_{4-x}\text{Ce}_{0.8}\text{Sm}_{0.2}\text{O}_{1.9}$  复合材料的物理和电化学性能起着关键作用。其中， $\text{FeCo}_2\text{O}_{4-60}\text{Ce}_{0.8}\text{Sm}_{0.2}\text{O}_{1.9}$  复合阴极在  $800^\circ\text{C}$  下具有最好的电催化活性，峰值功率密度为  $397\text{mW}\cdot\text{cm}^{-2}$ ，在空气中的极化电阻为  $0.094\Omega\cdot\text{cm}^2$ ，远小于  $\text{FeCo}_2\text{O}_4$  阴极的极化电阻  $4.18\Omega\cdot\text{cm}^2$ ，如图 6 所示。这种电化学性能的显著改善主要是由于反应活性区的延伸和氧化物离子电导率的增加。

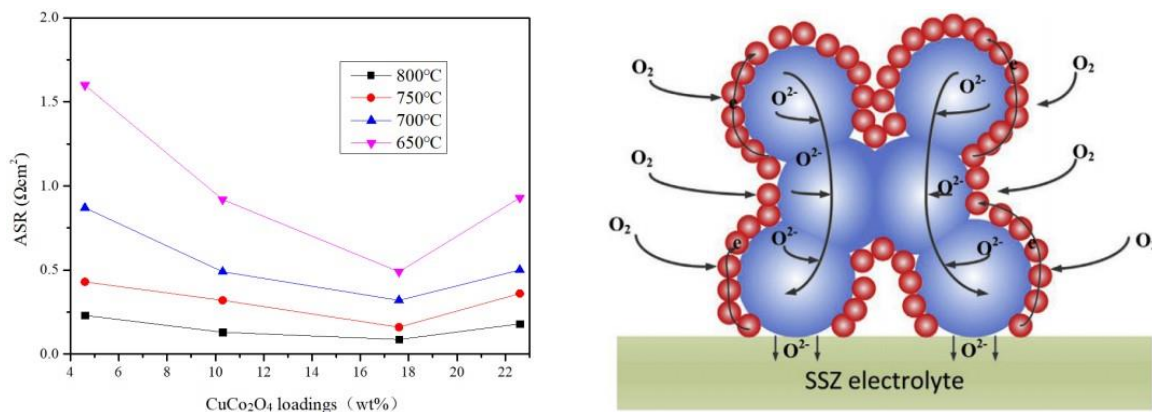


图 5. 浸渍  $\text{CuCo}_2\text{O}_4$  阴极的 ASR 及其结构示意图<sup>[70]</sup>

Fig 5. ASR of impregnated  $\text{CuCo}_2\text{O}_4$  cathode and its structure diagram<sup>[70]</sup>

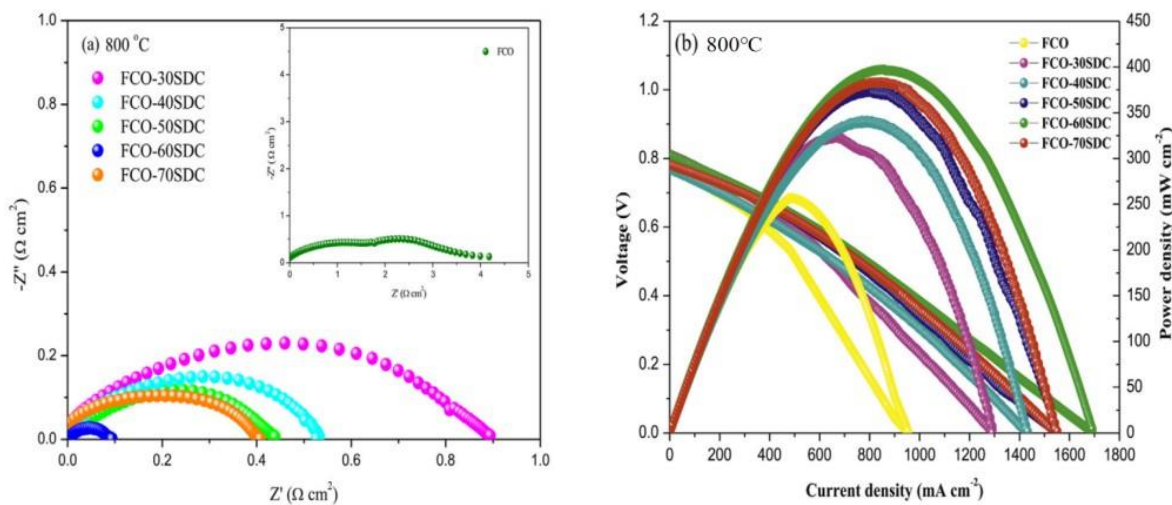


图 6. (a)  $\text{FCO-xSDC|SDC|FCO-xSDC}$  ( $x=0、30、40、50、60、70\text{wt.}\%$ ) 对称电池的电化学阻抗谱；(b)  $\sim 400\mu\text{m}$  SDC 电解质支撑的  $\text{FCO-xSDC}$  ( $x=0、30、40、50、60、70\text{wt.}\%$ ) 复合阴极的放电曲线（干  $\text{H}_2$  为燃料；空气为氧化剂）<sup>[39]</sup>

Fig 6. (a) The electrochemical impedance spectroscopy of  $\text{FCO-xSDC|SDC|FCO-xSDC}$  ( $x=0、30、40、50、60、70\text{wt.}\%$ ) symmetry battery; (b) Discharge curve of  $\text{FCO-xSDC}$  ( $x=0、30、40、50、60、70\text{wt.}\%$ ) composite cathode supported by  $\sim 400\mu\text{m}$  SDC electrolyte (dry  $\text{H}_2$  as fuel; Air as oxidant) <sup>[39]</sup>

### 2.3 Ruddlesden-popper 型结构



Ruddlesden-popper (R-P) 型结构材料可以用  $(\text{ABO}_3)_n\text{AO}$  (A=稀土/碱金属元素; B=过渡金属元素) 来表示, 其结构可以看做是  $n$  层四方钙钛矿  $(\text{ABO}_3)_n$  与  $\text{AO}$  交互层叠排列, 如图 1 (c) 所示。这种材料具有较高的氧扩散系数和表面交换系数, 显著提高了阴极材料的活性。最常用的体系是  $n=1$  的相, 它具有典型的  $\text{K}_2\text{NiF}_4$  结构。例如,  $\text{La}_2\text{NiO}_{4+\delta}$  就具有这种典型的结构特性, 具有良好的电化学催化活性, 但其与电解质的兼容性比较差,  $900^\circ\text{C}$  时,  $\text{La}_2\text{NiO}_{4+\delta}$  与 GDC 电解质有明显的化学反应<sup>[71-78]</sup>。据报道通过 La 位或 Ni 位的取代可以优化这个体系<sup>[79-81]</sup>。例如, Sr 和 Co 双掺杂的  $\text{La}_{2-x}\text{Sr}_x\text{Ni}_{1-x}\text{Co}_x\text{O}_{4+\delta}$  阴极具有优异的电化学性能。Zheng 等人提出用软化学法合成  $\text{La}_2\text{Ni}_{0.5}\text{Cu}_{0.5}\text{O}_4$  和  $\text{Pr}_2\text{Ni}_{0.5}\text{Cu}_{0.5}\text{O}_4$  氧化物作为 SOFC 阴极材料,  $\text{La}_2\text{Ni}_{0.5}\text{Cu}_{0.5}\text{O}_4$  和  $\text{Pr}_2\text{Ni}_{0.5}\text{Cu}_{0.5}\text{O}_4$  阴极的 TEC 分别为  $(10.0-13.5) \times 10^{-6}\text{K}^{-1}$  和  $(9.0-11.2) \times 10^{-6}\text{K}^{-1}$ , 与常用的电解质  $\text{La}_{0.9}\text{Sr}_{0.1}\text{Ga}_{0.8}\text{Mg}_{0.2}\text{O}_{2.85}$  ( $12.2 \times 10^{-6}\text{K}^{-1}$ )、 $\text{Ce}_{0.8}\text{Gd}_{0.2}\text{O}_{1.9}$  ( $12.5 \times 10^{-6}\text{K}^{-1}$ ) 等拥有较好的相容性<sup>[82]</sup>。在  $300\sim 800^\circ\text{C}$  范围内,  $\text{Pr}_2\text{Ni}_{0.5}\text{Cu}_{0.5}\text{O}_4$  阴极的电导率都超过  $100\text{S}\cdot\text{cm}^{-1}$ , 特别是在  $450^\circ\text{C}$  时, 电导率有最大值  $130\text{S}\cdot\text{cm}^{-1}$ , 如图 7 所示。以  $\text{Pr}_2\text{Ni}_{0.5}\text{Cu}_{0.5}\text{O}_4$  为阴极制备的  $\text{Pr}_2\text{Ni}_{0.5}\text{Cu}_{0.5}\text{O}_4|\text{Ce}_{0.8}\text{Gd}_{0.2}\text{O}_{1.9}|\text{Ni}-8\text{YSZ}$  电池在  $800^\circ\text{C}$  时的最大功率密度为  $130\text{mW}\cdot\text{cm}^{-2}$ 。Garali 等人采用机械球磨法合成了 Eu 掺杂的  $\text{La}_{2-x}\text{Eu}_x\text{NiO}_{4+\delta}$  ( $x=0, 0.2, 0.4, 0.6, 0.8$ ) ( $\text{LENO}_x$ ) 材料<sup>[83]</sup>。研究发现,  $\text{LENO}_x|\text{SDC}|\text{LENO}_x$  对称电池在空气中的  $R_p$  与 Eu 的掺杂量有关。当  $\text{Eu}=0.2$  时,  $700^\circ\text{C}$  下  $\text{LENO}_{0.2}$  的  $R_p$  有最小值  $1.3\Omega\cdot\text{cm}^2$ , 如图 8 所示。

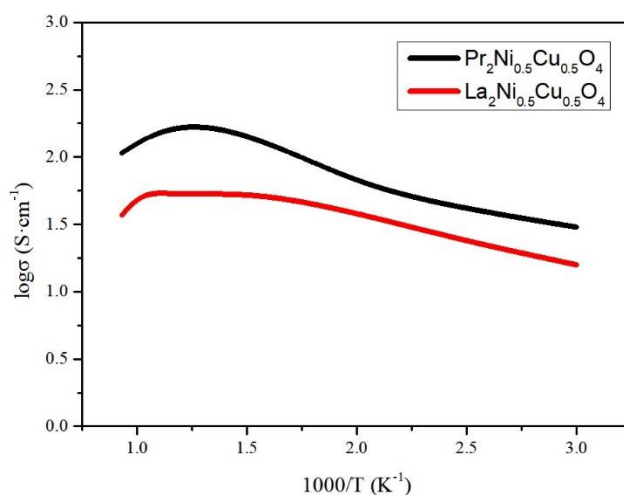


图 7. LNC 和 PNC 阴极电导率与温度的关系<sup>[82]</sup>

Fig 7. Relationship between cathode conductivity and temperature of LNC and PNC<sup>[82]</sup>

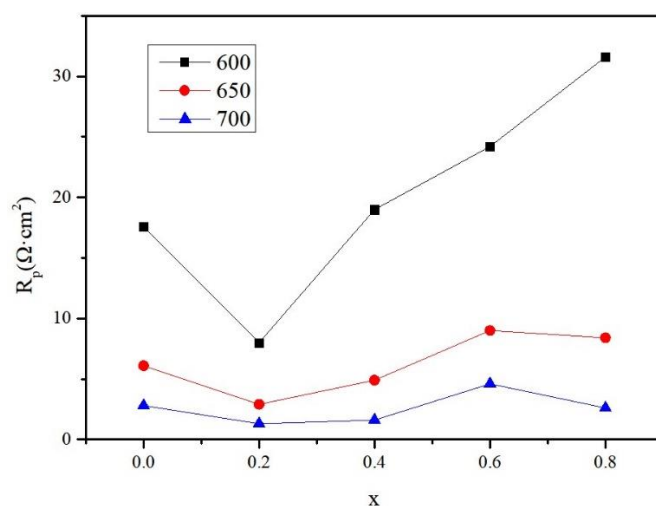


图 8.  $\text{LENO}_x|\text{SDC}|\text{LENO}_x$  对称电池的极化电阻和 Eu 掺杂量  $x$  的关系<sup>[83]</sup>

Fig 8. Relationship between polarization resistance and Eu doping amount  $x$  of  $\text{LENO}_x|\text{SDC}|\text{LENO}_x$  symmetrical cell<sup>[83]</sup>

### 3 结论与展望

SOFC 是一种将化学能直接转化为电能的能源转换装置，是解决能源紧缺问题的重要技术。多孔阴极是 SOFC 的重要结构，因此研究 SOFC 低温运行时性能优良的阴极材料是延长电池寿命、降低电池成本的关键。研究较多的  $\text{LaMnO}_3$  基阴极、 $\text{LaCoO}_3$  基阴极和  $\text{LaFeO}_3$  基阴极材料都属于钙钛矿结构氧化物，它们的电化学催化活性大小为： $\text{LaFeO}_3 < \text{LaMnO}_3 < \text{LaCoO}_3$ 。钙钛矿结构阴极材料的电子、离子电导性受掺杂剂的影响较大，A 位掺杂（如  $\text{Sr}^{2+}$ ）可以提高材料的离子电导率，B 位掺杂（如 Co）可以提高材料的电子导电性。此外，还有尖晶石结构阴极和 Ruddlesden-popper 型结构阴极材料，都具备优良的氧扩散性能和电化学活性，也是研究较多的 SOFC 阴极材料，拥有良好的研发潜力。综上可知，具备良好的电子/离子电导率、催化活性和氧扩散性能等优点的阴极及其复合材料，必然是 SOFC 阴极材料的研究焦点。

#### 参考文献：

- [1] Kober T, Schiffer H W, Densing M, et al. Global energy perspectives to 2060 – WEC’ s World Energy Scenarios 2019 [J]. Energy Strategy Reviews, 2020, 31: 100523.
- [2] Engels A, Kunkis M, Altstaedt S. A new energy world in the making: Imaginary business futures in a dramatically changing world of decarbonized energy production [J]. Energy research and social science, 2020, 60: 101321.
- [3] Mbungu N T, Naidoo R M, Bansal R C, et al. An overview of renewable energy resources and grid integration for commercial building applications [J]. Journal of Energy Storage, 2020, 29: 101385.
- [4] Ulucak R, Danish, Ozcan B. Relationship between energy consumption and environmental sustainability in OECD countries: The role of natural resources rents [J]. Resources Policy, 2020, 69: 101803.
- [5] Li Y, Yang J, Song J. Nano energy system model and nanoscale effect of graphene battery in renewable energy

- electric vehicle [J]. *Renewable and Sustainable Energy Reviews*, 2017, 69: 652-663.
- [6] Kendall M. Fuel cell development for New Energy Vehicles (NEVs) and clean air in China [J]. *Progress in Natural Science: Materials International*, 2018, 28(2): 113-120.
- [7] Wu H, Xiao J, Zeng X, et al. A high performance direct carbon solid oxide fuel cell – A green pathway for brown coal utilization [J]. *Applied Energy*, 2019, 248: 679-687.
- [8] Ramadhani F, Hussain M A, Mokhlis H, et al. Optimal heat recovery using photovoltaic thermal and thermoelectric generator for solid oxide fuel cell-based polygeneration system: Techno-economic and environmental assessments [J]. *Applied Thermal Engineering*, 2020, 181: 116015.
- [9] Dziurdzia B, Magoński Z, Jankowski H. Commercialisation of Solid Oxide Fuel Cells - opportunities and forecasts [J]. *IOP Conference Series: Materials Science and Engineering*, 2016, 104: 012020.
- [10] Irshad M, Siraj K, Raza R, et al. A Brief Description of High Temperature Solid Oxide Fuel Cell's Operation, Materials, Design, Fabrication Technologies and Performance [J]. *Applied Sciences*, 2016, 6(3): 1-23.
- [11] Silva F S D, De Souza T M. Novel materials for solid oxide fuel cell technologies: A literature review [J]. *International Journal of Hydrogen Energy*, 2017, 42(41): 26020-26036.
- [12] Chelmehsara M E, Mahmoudimehr J. Techno-economic comparison of anode-supported, cathode-supported, and electrolyte-supported SOFCs [J]. *International Journal of Hydrogen Energy*, 2018, 43(32): 15521-15530.
- [13] Futamura S, Muramoto A, Tachikawa Y, et al. SOFC anodes impregnated with noble metal catalyst nanoparticles for high fuel utilization [J]. *International Journal of Hydrogen Energy*, 2019, 44(16): 8502-8518.
- [14] Wainmartin A, Moranruiz A, Lagunabercero M A, et al. SOFC cathodic layers using wet powder spraying technique with self synthesized nanopowders [J]. *International Journal of Hydrogen Energy*, 2019, 44(14): 7555-7563.
- [15] Gao Z, Mogni L, Miller E C, et al. A perspective on low-temperature solid oxide fuel cells [J]. *Energy and Environmental Science*, 2016, 9(5): 1602-1644.
- [16] Seyedvakili S V, Babaei A, Ataie M, et al. Enhanced performance of  $\text{La}_{0.8}\text{Sr}_{0.2}\text{MnO}_3$  cathode for solid oxide fuel cells by co-infiltration of metal and ceramic precursors [J]. *Journal of Alloys and Compounds*, 2018, 737: 433-441.
- [17] Xu H, Chen B, Tan P, et al. Modeling of all porous solid oxide fuel cells [J]. *Applied Energy*, 2018, 219: 105-113.
- [18] Xu H, Chen B, Tan P, et al. Modeling of all-porous solid oxide fuel cells with a focus on the electrolyte porosity design [J]. *Applied Energy*, 2019, 235: 602-611.
- [19] Kan W H, Samson A J, Thangadurai V. Trends in electrode development for next generation solid oxide fuel cells [J]. *Journal of Materials Chemistry*, 2016, 4(46): 17913-17932.
- [20] Connor P A, Yue X, Savaniu C, et al. Tailoring SOFC Electrode Microstructures for Improved Performance [J]. *Advanced Energy Materials*, 2018, 8(23): 1800120.
- [21] Choi H J, Bae K, Grieshammer S, et al. Surface Tuning of Solid Oxide Fuel Cell Cathode by Atomic Layer Deposition [J]. *Advanced Energy Materials*, 2018, 8(33): 1802506.
- [22] Su H, Hu Y H. Progress in low-temperature solid oxide fuel cells with hydrocarbon fuels [J]. *Chemical Engineering Journal*, 2020, 402: 126235.
- [23] Shu L, Sunarso J, Hashim S S, et al. Advanced perovskite anodes for solid oxide fuel cells: A review [J]. *International Journal of Hydrogen Energy*, 2019, 44(59): 31275-31304.
- [24] Sreedhar I, Agarwal B, Goyal P, et al. Recent advances in material and performance aspects of solid oxide fuel cells [J]. *Journal of Electroanalytical Chemistry*, 2019, 848: 113315.
- [25] Silva-Mosqueda D M, Elizalde-Blancas F, Pumiglia D, et al. Intermediate temperature solid oxide fuel cell under internal reforming: Critical operating conditions, associated problems and their impact on the performance [J].

Applied Energy, 2019, 235: 625-640.

- [26] Lu Y, Cai Y, Souamy L, et al. Solid oxide fuel cell technology for sustainable development in China: An overview [J]. International Journal of Hydrogen Energy, 2018, 43(28): 12870-12891.
- [27] Wu C, Yang Z, Huo S, et al. Modeling and optimization of electrode structure design for solid oxide fuel cell [J]. International Journal of Hydrogen Energy, 2018, 43(31): 14648-14664.
- [28] Wang Y, Leung D Y C, Xuan J, et al. A review on unitized regenerative fuel cell technologies, part B: Unitized regenerative alkaline fuel cell, solid oxide fuel cell, and microfluidic fuel cell [J]. Renewable and Sustainable Energy Reviews, 2017, 75: 775-795.
- [29] Da Silva F S, De Souza T M. Novel materials for solid oxide fuel cell technologies: A literature review [J]. International Journal of Hydrogen Energy, 2017, 42(41): 26020-26036.
- [30] Dogdibegovic E, Wang R, Lau G Y, et al. High performance metal-supported solid oxide fuel cells with infiltrated electrodes [J]. Journal of Power Sources, 2019, 410-411: 91-98.
- [31] Abd Aziz A J, Baharuddin N A, Somalu M R, et al. Review of composite cathodes for intermediate-temperature solid oxide fuel cell applications [J]. Ceramics International, 2020, 46(15): 23314-23325.
- [32] Anasuhah W, Yusoff W, Wardah N, et al. Fabrication Process of Cathode Materials for Solid Oxide Fuel Cells [J]. Journal of Advanced Research in Fluid Mechanics and Thermal Sciences, 2018, 50: 153-160.
- [33] Cheng J, Wang Z, Zou L, et al. Doping optimization mechanism of a bi-functional perovskite catalyst  $\text{La}_{0.8}\text{Sr}_{0.2}\text{Co}_{0.8}\text{Ni}_{0.2}\text{O}_{3-\delta}$  for Li-O<sub>2</sub> battery cathode [J]. Journal of Alloys and Compounds, 2020, 831: 154728.
- [34] Kaur P, Singh K. Review of perovskite-structure related cathode materials for solid oxide fuel cells [J]. Ceramics International, 2020, 46(5): 5521-5535.
- [35] Xu X, Zhao J, Li M, et al. Sc and Ta-doped  $\text{SrCoO}_{3-\delta}$  perovskite as a high-performance cathode for solid oxide fuel cells [J]. Composites Part B: Engineering, 2019, 178: 107491.
- [36] Xia W, Li Q, Sun L, et al. Electrochemical performance of Sn-doped  $\text{Bi}_{0.5}\text{Sr}_{0.5}\text{FeO}_{3-\delta}$  perovskite as cathode electrocatalyst for solid oxide fuel cells [J]. Journal of Alloys and Compounds, 2020, 835: 155406.
- [37] Xin X, Liu L, Liu Y, et al. Novel perovskite-spinel composite conductive ceramics for SOFC cathode contact layer [J]. International Journal of Hydrogen Energy, 2018, 43(51): 23036-23040.
- [38] Mushtaq N, Xia C, Dong W, et al. Perovskite  $\text{SrFe}_{1-x}\text{Ti}_x\text{O}_{3-\delta}$  ( $x \leq 0.1$ ) cathode for low temperature solid oxide fuel cell [J]. Ceramics International, 2018, 44(9): 10266-10272.
- [39] Li H, Su C, Wang C, et al. Electrochemical performance evaluation of  $\text{FeCo}_2\text{O}_4$  spinel composite cathode for solid oxide fuel cells [J]. Journal of Alloys and Compounds, 2020, 829: 154493.
- [40] Zhen S, Sun W, Li P, et al. High performance cobalt-free  $\text{Cu}_{1.4}\text{Mn}_{1.6}\text{O}_4$  spinel oxide as an intermediate temperature solid oxide fuel cell cathode [J]. Journal of Power Sources, 2016, 315: 140-144.
- [41] Zhou Q, Zhang T, Zhao C, et al. Electrochemical properties of  $\text{La}_{1.5}\text{Pr}_{0.5}\text{Ni}_{0.95-x}\text{Cu}_x\text{Al}_{0.05}\text{O}_{4+\delta}$  Ruddlesden-Popper phase as cathodes for intermediate-temperature solid oxide fuel cells [J]. Materials Research Bulletin, 2020, 131: 110986.
- [42] Miao L, Hou J, Gong Z, et al. A high-performance cobalt-free Ruddlesden-Popper phase cathode  $\text{La}_{1.2}\text{Sr}_{0.8}\text{Ni}_{0.6}\text{Fe}_{0.4}\text{O}_{4+\delta}$  for low temperature proton-conducting solid oxide fuel cells [J]. International Journal of Hydrogen Energy, 2019, 44(14): 7531-7537.
- [43] Yattoo M A, Du Z, Zhao H, et al.  $\text{La}_2\text{Pr}_2\text{Ni}_3\text{O}_{10\pm\delta}$  Ruddlesden-Popper phase as potential intermediate temperature-solid oxide fuel cell cathodes [J]. Solid State Ionics, 2018, 320: 148-151.
- [44] Chaianansutcharit S, Ju Y W, Ida S, et al. Ni doped  $\text{PrSr}_3\text{Fe}_3\text{O}_{10-\delta}$  Ruddlesden-Popper oxide for active oxygen reduction cathode for solid oxide fuel cell [J]. Electrochimica Acta, 2016, 222: 1853-1860.
- [45] Irshad M, Idrees R, Siraj K, et al. Electrochemical evaluation of mixed ionic electronic perovskite cathode  $\text{LaNi}_{1-x}\text{Co}_x\text{O}_{3-\delta}$  for IT-SOFC synthesized by high temperature decomposition [J]. International Journal of Hydrogen

Energy, 2021, 46(17): 10448-10456.

- [46] Shimada H, Yamaguchi T, Sumi H, et al. Extremely fine structured cathode for solid oxide fuel cells using Sr-doped LaMnO<sub>3</sub> and Y<sub>2</sub>O<sub>3</sub>-stabilized ZrO<sub>2</sub> nano-composite powder synthesized by spray pyrolysis [J]. *Journal of Power Sources*, 2017, 341: 280-284.
- [47] Zeng R, Huang Y. High-performance low-temperature solid oxide fuel cells prepared by sol impregnation [J]. *Journal of Alloys and Compounds*, 2019, 810: 151936.
- [48] Wang H, Zhang X, Zhang W, et al. Enhancing catalysis activity of La<sub>0.6</sub>Sr<sub>0.4</sub>Co<sub>0.8</sub>Fe<sub>0.2</sub>O<sub>3-δ</sub> cathode for solid oxide fuel cell by a facile and efficient impregnation process [J]. *International Journal of Hydrogen Energy*, 2019, 44(26): 13757-13767.
- [49] Osinkin D A, Bogdanovich N M, Beresnev S M, et al. High-performance anode-supported solid oxide fuel cell with impregnated electrodes [J]. *Journal of Power Sources*, 2015, 288: 20-25.
- [50] Koo J Y, Mun T, Lee J, et al. Enhancement of oxygen reduction reaction kinetics using infiltrated yttria-stabilized zirconia interlayers at the electrolyte/electrode interfaces of solid oxide fuel cells [J]. *Journal of Power Sources*, 2020, 472: 228606.
- [51] Ovtar S, Hauch A, Veltzé S, et al. Comparison between La<sub>0.6</sub>Sr<sub>0.4</sub>CoO<sub>3-d</sub> and LaNi<sub>0.6</sub>Co<sub>0.4</sub>O<sub>3-d</sub> infiltrated oxygen electrodes for long-term durable solid oxide fuel cells [J]. *Electrochimica Acta*, 2018, 266: 293-304.
- [52] Brito M E, Morishita H, Yamada J, et al. Further improvement in performances of La<sub>0.6</sub>Sr<sub>0.4</sub>Co<sub>0.2</sub>Fe<sub>0.8</sub>O<sub>3-δ</sub>-doped ceria composite oxygen electrodes with infiltrated doped ceria nanoparticles for reversible solid oxide cells [J]. *Journal of Power Sources*, 2019, 427: 293-298.
- [53] Ju J, Lin J, Wang Y, et al. Electrical performance of nanostructured strontium-doped lanthanum manganite impregnated onto yttria-stabilized zirconia backbone [J]. *Journal of Power Sources*, 2016, 302: 298-307.
- [54] Develos-Bagarinao K, De Vero J, Kishimoto H, et al. Multilayered LSC and GDC: An approach for designing cathode materials with superior oxygen exchange properties for solid oxide fuel cells [J]. *Nano Energy*, 2018, 52: 369-380.
- [55] Khan M Z, Song R-H, Mehran M T, et al. Controlling cation migration and inter-diffusion across cathode/interlayer/electrolyte interfaces of solid oxide fuel cells: A review [J]. *Ceramics International*, 2021, 47(5): 5839-5869.
- [56] Xu H, Sun K, Cheng J, et al. Improved stability of nano-sized La<sub>0.6</sub>Sr<sub>0.4</sub>Co<sub>0.2</sub>Fe<sub>0.8</sub>O<sub>3-δ</sub>-Ce<sub>0.8</sub>Sm<sub>0.2</sub>O<sub>1.9</sub> composite cathodes by substituting Sr<sup>2+</sup> with Ca<sup>2+</sup> [J]. *International Journal of Hydrogen Energy*, 2020, 45(35): 17717-17726.
- [57] Zhou F, Liu Y, Zhao X, et al. Effects of cerium doping on the performance of LSCF cathodes for intermediate temperature solid oxide fuel cells [J]. *International Journal of Hydrogen Energy*, 2018, 43(41): 18946-18954.
- [58] Dos Santos-Gómez L, Porras-Vázquez J M, Losilla E R, et al. Stability and performance of La<sub>0.6</sub>Sr<sub>0.4</sub>Co<sub>0.2</sub>Fe<sub>0.8</sub>O<sub>3-δ</sub> nanostructured cathodes with Ce<sub>0.8</sub>Gd<sub>0.2</sub>O<sub>1.9</sub> surface coating [J]. *Journal of Power Sources*, 2017, 347: 178-185.
- [59] Xi X, Kondo A, Kozawa T, et al. LSCF-GDC composite particles for solid oxide fuel cells cathodes prepared by facile mechanical method [J]. *Advanced Powder Technology*, 2016, 27(2): 646-651.
- [60] Li G, He B, Ling Y, et al. Highly active YSB infiltrated LSCF cathode for proton conducting solid oxide fuel cells [J]. *International Journal of Hydrogen Energy*, 2015, 40(39): 13576-13582.
- [61] Ben Mya O, Dos Santos-Gómez L, Porras-Vázquez J M, et al. La<sub>1-x</sub>Sr<sub>x</sub>Fe<sub>0.7</sub>Ni<sub>0.3</sub>O<sub>3-δ</sub> as both cathode and anode materials for Solid Oxide Fuel Cells [J]. *International Journal of Hydrogen Energy*, 2017, 42(36): 23160-23169.
- [62] Hansen K K. Evaluation of LSF based SOFC cathodes using cone-shaped electrodes and EIS [J]. *Solid State Ionics*, 2020, 344: 115096.
- [63] Shao L, Wang Q, Fan L, et al. Copper cobalt spinel as a high performance cathode for intermediate temperature

- solid oxide fuel cells [J]. *Chemical Communications*, 2016, 52(55): 8615-8618.
- [64] Luo X, Ben L. Effect of MgO and Ta<sub>2</sub>O<sub>5</sub> co-coatings on electrochemical performance of high-voltage spinel LiNi<sub>0.5</sub>Mn<sub>1.5</sub>O<sub>4</sub> cathode material [J]. *Journal of Alloys and Compounds*, 2019, 810: 151951.
- [65] Yu Y T, Zhu J H, Bates B L. Conductive spinels derived from Co-Mn based alloy precursor for SOFC cathode-side contact application [J]. *International Journal of Hydrogen Energy*, 2020, 45(51): 27745-27753.
- [66] Wang R, Sun Z, Pal U B, et al. Mitigation of chromium poisoning of cathodes in solid oxide fuel cells employing CuMn<sub>1.8</sub>O<sub>4</sub> spinel coating on metallic interconnect [J]. *Journal of Power Sources*, 2018, 376: 100-110.
- [67] Shao L, Chen G-D, Si F-Z, et al. One-step synthesis of CuCo<sub>2</sub>O<sub>4</sub>-Sm<sub>0.2</sub>Ce<sub>0.8</sub>O<sub>1.9</sub> nanofibers as high performance composite cathodes of intermediate-temperature solid oxide fuel cells [J]. *International Journal of Hydrogen Energy*, 2020, 45(22): 12577-12582.
- [68] Gao J-T, Li J-H, Feng Q-Y, et al. High performance of ceramic current collector fabricated at 550°C through in-situ joining of reduced Mn<sub>1.5</sub>Co<sub>1.5</sub>O<sub>4</sub> for metal-supported solid oxide fuel cells [J]. *International Journal of Hydrogen Energy*, 2020, 45(53): 29123-29130.
- [69] Zhang L, Li D, Zhang S. One-step synthesized Co<sub>1.5</sub>Mn<sub>1.5</sub>O<sub>4</sub>-Ce<sub>0.8</sub>Sm<sub>0.2</sub>O<sub>1.9</sub> composite cathode material for intermediate temperature solid oxide fuel cells [J]. *Ceramics International*, 2017, 43(2): 2859-2863.
- [70] Shao L, Wang P, Zhang Q, et al. Nanostructured CuCo<sub>2</sub>O<sub>4</sub> cathode for intermediate temperature solid oxide fuel cells via an impregnation technique [J]. *Journal of Power Sources*, 2017, 343: 268-274.
- [71] Li J, Liu B, Jia L, et al. Investigation on the oxygen reduction reaction mechanism of PrBa<sub>0.5</sub>Sr<sub>0.5</sub>Co<sub>1.5</sub>Fe<sub>0.5</sub>O<sub>5+δ</sub>@La<sub>2</sub>NiO<sub>4+δ</sub> core-shell structure cathode for solid oxide fuel cells [J]. *International Journal of Hydrogen Energy*, 2019, 44(48): 26489-26497.
- [72] Lee Y, Kim H. Electrochemical performance of La<sub>2</sub>NiO<sub>4+δ</sub> cathode for intermediate-temperature solid oxide fuel cells [J]. *Ceramics International*, 2015, 41(4): 5984-5991.
- [73] Sharma R K, Burriel M, Dessemond L, et al. An innovative architectural design to enhance the electrochemical performance of La<sub>2</sub>NiO<sub>4+δ</sub> cathodes for solid oxide fuel cell applications [J]. *Journal of Power Sources*, 2016, 316: 17-28.
- [74] Schrödl N, Bucher E, Egger A, et al. Long-term stability of the IT-SOFC cathode materials La<sub>0.6</sub>Sr<sub>0.4</sub>CoO<sub>3-δ</sub> and La<sub>2</sub>NiO<sub>4+δ</sub> against combined chromium and silicon poisoning [J]. *Solid State Ionics*, 2015, 276: 62-71.
- [75] Wang Y-P, Zhao K, Xu Q, et al. Optimization on the electrochemical properties of La<sub>2</sub>NiO<sub>4+δ</sub> cathodes by tuning the cathode thickness [J]. *International Journal of Hydrogen Energy*, 2018, 43(9): 4482-4491.
- [76] Li P, Wang Z, Huang X, et al. Enhanced electrochemical performance of co-synthesized La<sub>2</sub>NiO<sub>4+δ</sub>-Ce<sub>0.55</sub>La<sub>0.45</sub>O<sub>2-δ</sub> composite cathode for IT-SOFCs [J]. *Journal of Alloys and Compounds*, 2017, 705: 105-111.
- [77] Jeong C, Lee J-H, Park M, et al. Design and processing parameters of La<sub>2</sub>NiO<sub>4+δ</sub>-based cathode for anode-supported planar solid oxide fuel cells (SOFCs) [J]. *Journal of Power Sources*, 2015, 297: 370-378.
- [78] Tong X, Zhou F, Yang S, et al. Performance and stability of Ruddlesden-Popper La<sub>2</sub>NiO<sub>4+δ</sub> oxygen electrodes under solid oxide electrolysis cell operation conditions [J]. *Ceramics International*, 2017, 43(14): 10927-10933.
- [79] Li X, Huan D, Shi N, et al. Defects evolution of Ca doped La<sub>2</sub>NiO<sub>4+δ</sub> and its impact on cathode performance in proton-conducting solid oxide fuel cells [J]. *International Journal of Hydrogen Energy*, 2020, 45(35): 17736-17744.
- [80] Gu C-Y, Wu X-S, Cao J-F, et al. High performance Ca-containing La<sub>2-x</sub>Ca<sub>x</sub>NiO<sub>4+δ</sub> (0≤x≤0.75) cathode for proton-conducting solid oxide fuel cells [J]. *International Journal of Hydrogen Energy*, 2020, 45(43): 23422-23432.
- [81] Akbari-Fakhrabadi A, Toledo E G, Canales J I, et al. Effect of Sr<sup>2+</sup> and Ba<sup>2+</sup> doping on structural stability and mechanical properties of La<sub>2</sub>NiO<sub>4+δ</sub> [J]. *Ceramics International*, 2018, 44(9): 10551-10557.
- [82] Zheng K, Świerczek K. Evaluation of La<sub>2</sub>Ni<sub>0.5</sub>Cu<sub>0.5</sub>O<sub>4+δ</sub> and Pr<sub>2</sub>Ni<sub>0.5</sub>Cu<sub>0.5</sub>O<sub>4+δ</sub> Ruddlesden-Popper-type layered oxides as cathode materials for solid oxide fuel cells [J]. *Materials Research Bulletin*, 2016, 84: 259-266.



[83] Garali M, Kahlaoui M, Mohammed B, et al. Synthesis, characterization and electrochemical properties of  $\text{La}_{2-x}\text{Eu}_x\text{NiO}_{4+\delta}$  Ruddlesden-Popper-type layered nickelates as cathode materials for SOFC applications [J]. International Journal of Hydrogen Energy, 2019, 44(21): 11020-11032.

## Research progress of cathode materials in solid oxide fuel cells

Fengjie Shang<sup>1</sup>, Qinlan Li<sup>1</sup>, Yongjing Shi<sup>1</sup>, Wei Dai<sup>1</sup>, Haiding Liu<sup>2</sup>, Shigeng Song<sup>3</sup>

(1. School of Metallurgy and Materials Engineering, Chongqing University of Science and Technology, Chongqing 401331, China; 2. Chongqing material Research Institute Co., Ltd, Chongqing 401331, China; 3. Institute of Thin Films, Sensors and Imaging, School of Engineering and Computing, University of the West of Scotland, Paisley PA1 2BE, UK)

**Abstract:** Cathode material is an important component of solid oxide fuel cell. Improving the electron / ion conductivity of cathode materials and reducing the polarization resistance are important methods to make SOFC operate at low temperature and increase the service life of battery. The high electronic conductivity of cathode materials makes perovskite oxides occupy a dominant position in the research field of cathode materials. In this paper, the research progress of perovskite structure cathode, spinel structure cathode and Ruddlesden-popper structure cathode materials was reviewed, and the development direction of cathode materials in the future was prospected.

**Keywords:** Solid Oxide Fuel Cell (SOFC); Cathode materials; perovskite oxides; Research progress